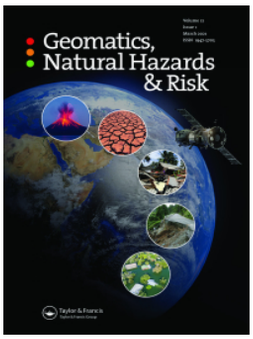

Geomatics, Natural Hazards and Risk

ISSN: 1947-5705 (Print) 1947-5713 (Online) Journal homepage: www.tandfonline.com/journals/tgnh20

Machine learning-based assessment of flood susceptibility in the Eastern Mediterranean: a case study of Baniyas River basin

Hazem Ghassan Abdo, Sahar Mohammed Richi, Taorui Zeng , Saeed Alqadhi , Pankaj Prasad , Thong Nguyen-Huy , Maged Muteb Alharbi & Javed Mallick

To cite this article: Hazem Ghassan Abdo, Sahar Mohammed Richi, Taorui Zeng , Saeed Alqadhi , Pankaj Prasad , Thong Nguyen-Huy , Maged Muteb Alharbi & Javed Mallick (2025) Machine learning-based assessment of flood susceptibility in the Eastern Mediterranean: a case study of Baniyas River basin, Geomatics, Natural Hazards and Risk, 16:1, 2524417, DOI: 10.1080/19475705.2025.2524417

To link to this article: https://doi.org/10.1080/19475705.2025.2524417

Published online: 01 Jul 2025.

GEOMATICS, NATURAL HAZARDS AND RISK
2025, VOL. 16, NO. 1, 2524417
https://doi.org/10.1080/19475705.2025.2524417

Machine learning-based assessment of flood susceptibility in the Eastern Mediterranean: a case study of Baniyas River basin

Hazem Ghassan Abdo[a], Sahar Mohammed Richi[a], Taorui Zeng[b,c], Saeed Alqadhi[d], Pankaj Prasad[e], Thong Nguyen-Huy[f,g], Maged Muteb Alharbi[h] and Javed Mallick[d]

[a]Geography Department, Faculty of Arts and Humanities, Tartous University, Tartous, Syria; [b]Institute of Future Civil Engineering Science and Technology, Chongqing Jiaotong University, Chongqing, China; [c]Institute of Frontier Interdisciplinary Technology, Chongqing Jiaotong University, Chongqing, China; [d]Department of Civil Engineering, College of Engineering, King Khalid University, Abha, Kingdom of Saudi Arabia; [e]Geoinformatics Division, Department of Geography, Mahapurusha Srimanta Sankaradeva Viswavidyalaya, Nagaon, India; [f]Centre for Applied Climate Sciences, University of Southern Queensland, Toowoomba, QLD, Australia; [g]Faculty of Information Technology, Thanh Do University, Kim Chung, Hoai Duc, Ha Noi, Vietnam; [h]Ministry of Environment, Water and Agriculture, Saudi Irrigation Organization, Riyadh, Kingdom of Saudi Arabia

ABSTRACT

Floods are one of the main damaging physical catastrophes, inducing economic losses and human casualties worldwide. The Eastern Mediterranean region is exposed to devastating flood events annually, with catastrophic consequences due to the complexity of the physical and human geographical characteristics. In this analysis, the performance of four ensemble machine learning algorithms (ML), that is support vector machine (SVM), random forest (RF), artificial neural network (ANN) and extreme gradient boost (XGBoost), was compared and tested in mapping flood susceptibility in the Eastern Mediterranean region. In the Baniyas River basin in western Syria, 1,100 flood events with 20 flood-driving factors were relied upon to achieve the goal of this assessment. The multicollinearity test results showed that all selected factors can be incorporated into the modelling process. Additionally, all the applied algorithms showed reliable and accurate performance in modeling flood susceptibility; however, the XGBoost algorithm achieved the strongest performance compared to other models with an AUC value of 0.98. Overall, the current results guide urban planners and land managers in increasing the quality of sustainable development practices and enhancing community resilience to flood risk in the study area.

ARTICLE HISTORY
Received 18 November 2024
Accepted 19 June 2025

KEYWORDS
Flood susceptibility; machine learning; risk assessment; Baniyas River basin; Eastern Mediterranean

CONTACT Hazem Ghassan Abdo hazemabdo@tartous-univ.edu.sy

1. Introduction

A flood occurs when a river's natural bed is overflowing, submerging the surrounding area and causing significant harm to human life and property (Dutta et al. 2023; Al-Ruzouq et al. 2024; El-Aal et al. 2024; Ramadan et al. 2025). Therefore, spatial prediction of these natural hazards is so important that missing regions in a watershed vulnerable to flooding might worsen its disastrous impacts (Peresan and Hassan, 2024; Alogayell et al. 2024). The development of flood susceptibility maps, using Geographic Information Systems (GIS), machine learning (ML), and statistical models, is considered among the most important strategies that enable flood management. To successfully prepare these maps, though, one must have a solid grasp of the elements that contribute to flooding, be able to identify those factors, understand how each one affects flooding, and be able to choose and/or construct appropriate models. The degree of sensitivity to harm from dangerous water-related occurrences is known as flood susceptibility. Finding flood-prone locations is necessary for ensuring quick and efficient emergency response times and implementing appropriate land planning and management techniques (Samany et al. 2021). The creation of flood susceptibility maps has been effectively supported by the enhanced creation of flooding zones made possible by incorporating GIS into hydrological research (Sarkar et al. 2022). Recently, many methods and strategies for mapping flood susceptibility have been developed and tested (He et al. 2025). Various models have been combined with GIS and remote sensing data to estimate the degree of flooding susceptibility at a specific site (Costache et al. 2021). Several factors that affect the likelihood of flooding can be taken into account while using GIS.

The literature indicates that the development of flood susceptibility maps using several statistical and ML techniques has been the goal of many natural hazards scholars worldwide. Statistical techniques, such as frequency ratio, logistic regression, weights of evidence, and analytic hierarchy process (multiple criteria decision-making), are primarily predicated on the idea that past flood episodes are strongly associated with flood-purposing variables (Sarkar and Mondal 2020; Farhadi et al. 2022). In this regard, the analytic hierarchy process was not enough, so it was combined with fuzzy logic in several papers (Sepehri et al. 2020). Moreover, the superiority of ML models to statistical techniques for flood susceptibility mapping is presented (Nachappa et al. 2020). Recently, ML methods such as artificial neural networks (ANN), decision trees (DT), random forests (RF), and support vector machines (SVM) have been used to predict floods (Essam et al. 2022; Youssef et al. 2022; Yu et al. 2023; Badreldin et al., 2025).

Feature engineering is often a crucial step that produces an acceptable feature representation from the raw data (e.g. the pixel values of the picture) before data modelling when using an ML approach to address a specific problem. Furthermore, how the raw data are represented has a significant impact on how well ML techniques function (Kalantar et al. 2021; Zhang et al. 2021). In this regard, ML techniques are not able to directly extract informative representations from unprocessed data or derive fresh insights from these representations, which would enhance their prediction power. ML approaches have drawn a lot of attention recently due to their ability to produce dependable results that are either better than or on par with traditional techniques (Alzubaidi et al. 2021; Dawson and Lewin 2024). This approach covers a wide range of techniques with various network designs for computer vision, signal

processing, and natural language processing. Furthermore, flood susceptibility analysis has made use of several feature engineering techniques, including correlation-based, data acquisition ratio, and multi-collinearity assessment.

Mapping flood risk is fraught with difficulties. First of all, it might be difficult to choose non-occurrence flood spots using the appropriate strategy. Yes, there are several approaches, and they all provide distinct outcomes. Since no one model is universally agreed upon and each model has advantages and disadvantages of its own, choosing a model for flood susceptibility mapping is another problem. Based on its assumptions about data distribution, sensitivity to extreme values, internal characteristics, and the main drivers of development, each model may exhibit varying degrees of accuracy.

The Eastern Mediterranean region in general, and Syria in particular, is exposed to devastating annual flood events due to the outstanding topographical, climatic, and ecological factors (Alrawi et al. 2023; Özdemir et al. 2023; Abd-Elhamid et al. 2024; Badreldin et al., 2025). These floods cause catastrophic effects, especially the loss of lives and the destruction of property and infrastructure, especially in coastal areas in the west of Syria (Abdo 2020; Abd-Elhamid et al. 2024). These areas are characterized by significant human activity involving high population and urban density. Due to the region's high population density, extensive deforestation, and lack of governmental oversight over densely populated areas near rivers, the eastern Mediterranean has recently seen several severe floods. Continuous improvement of the quality of flood susceptibility maps is one of the most essential foundations for sound management of flood risk in the Eastern Mediterranean. Moreover, this investigation presents the first spatial assessment of flood vulnerability in Syria using the integration of ML algorithms and geospatial tools. The gap of this study is identified by the lack of application of ML algorithms in flood susceptibility modeling within regional contexts with 20 driving factors in the Eastern Mediterranean. Therefore, this analysis will provide a constructive perspective in enhancing the accuracy of flood susceptibility maps using ML and geospatial tools in the Eastern Mediterranean with a focus on the Banias River Basin. In this regard, this study presents a constructive approach for analyzing flood vulnerability using advanced ML algorithms in data-scarce regions. This will provide an objective and reliable method for data-poor regions around the world. Based on what was discussed above, the main objective of this article is to evaluate the influence of 20 geographical factors on flood risk, followed by testing the performance of widely-known ML models, such as SVM, RF, ANN, and Extreme Gradient Boost (XGBoost), in developing flood vulnerability maps in the Eastern Mediterranean.

2. Materials and methods

2.1. Study area

The Baniyas River Basin is located in the eastern basin of the Mediterranean, a part of the coastal region of Syria, spanning between Latitudes 35° 53′–36° 07′ North and Longitudes 35° 00′–35° 18′ East, and encompasses an area of 58.52 km^2 (Figure 1). This basin shares borders with the Mediterranean to the west, the Marqyah basin to the east, the Al-Basiah river basin to the south, and the Jober river basin to the north. Geologically, the lithological composition across the study area ranges from *Jurassic* to *Quaternary* formations. The study area can be divided into three primary

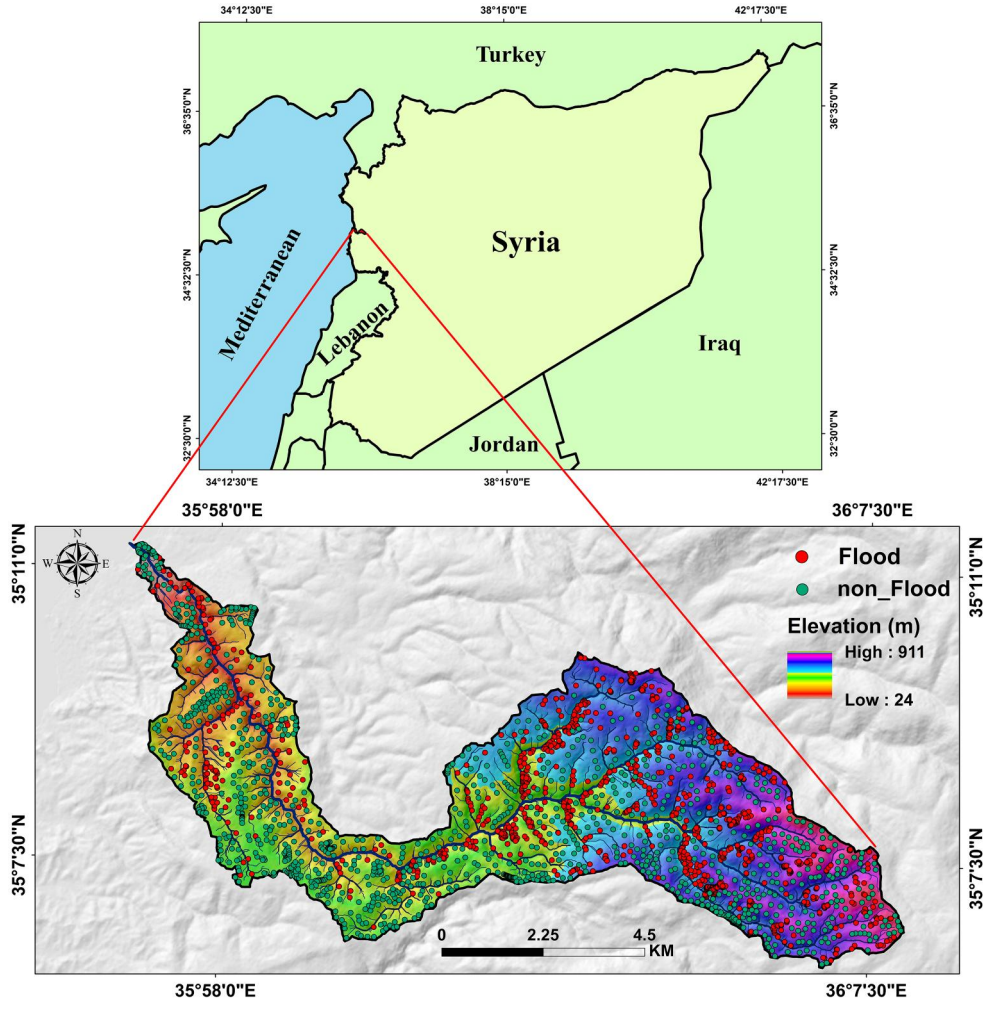

Figure 1. The study area location of the Baniyas River basin.

geomorphological patterns: the plain area (0–100 m). The hill area (100–400 m) primarily comprises upland regions with sloping valleys, while the dissected mountain area (400–911 m) is characterized by faulted walls, steep slopes, and narrow valleys, with various geomorphological processes, notably karstification. Predominantly, the study subbasin is located within the Mediterranean climate pattern with mild, rainy winters and long, dry, hot summers. Average temperatures reach 11.2 °C in winter and 23.8 °C in summer, while annual precipitation ranges between 1000 and 1300 mm (Alsafadi et al. 2021), peaking in January. This region falls within a wet-warm climate '*Csa*' category according to the *Köppen – Geiger* climate classification.

2.2. Flood inventory map

To effectively evaluate flood susceptibility in the Eastern Mediterranean region, the importance of the Flood Inventory Map is emphasized in this study. As an essential

tool, the map facilitates understanding flood occurrence patterns and frequencies in the region (Zeng et al. 2023). Analysis of historical flood data enables the creation of flood-prone areas, contributing significantly to a strong scientific basis for disaster management and urban planning strategies. The dataset was constructed utilizing a comprehensive methodology. Aligning with the demands of ML analysis, the research team meticulously chose a balanced number of flood and non-flood event samples, with each category comprising 1,100 samples, amounting to a total of 2,200.

This approach aims to bolster the model's capacity for generalization and accuracy in predictions, thereby solidifying the trustworthiness of the research outcomes (Zeng et al. 2023). Samples representing flood events were derived from documented historical occurrences, whereas non-flood samples included regions without recorded flooding incidents.

In this regard, the locations of flood events during the period 1991–2023 were identified based on an in-depth review of the historical records of the Directorate of Meteorology and the Directorate of Water Resources in Tartous Governorate, in addition to data derived from the archives of the Ministry of Agriculture in Damascus Governorate. In addition, the production of the inventory data included many field visits and community observations to fill the gaps in the inventory data and collect the largest possible number of inventory events. After collecting this data, the flood events were accurately digitized in the form of a point layer in the GIS environment. Flood events were identified based on the absence of their areas in the historical records, in addition to analyzing the driving factors of floods, including elevation, slope and distance from the river. Exploring the locations of non-floods was among the objectives of the fieldwork carried out.

Furthermore, the research methodology involved categorizing these samples into a training set, accounting for 70%, and a validation/test set, making up the remaining 30%. This segmentation ensures the model's resilience across various data scenarios (Zeng et al. 2023). The adopted distribution strategy reflects real-world complexity, enhancing the forecast accuracy for future flood events. Overall, this study, with its rigorously developed dataset and analytical techniques, strives to establish a robust scientific framework for accurately determining flood susceptibility in the Eastern Mediterranean region.

2.3. Data acquisition and preparation

The study conducted an exhaustive analysis of crucial topographical and hydrological factors to evaluate the risk of flooding in the Eastern Mediterranean region. Factors such as slope angle, slope aspect, various curvatures (including plan and profile), elevation, streams, and several indices including the Stream Power Index (SPI), Topographic Position Index (TPI), Terrain Ruggedness Index (TRI), Sediment Transport Index (STI), Flow Accumulation (FAc), and Topographic Wetness Index (TWI) were rigorously examined (Table 1). The primary data source for these factors was the Alaska Satellite Facility's (ASF) and Digital Elevation Model (DEM), specifically the ALOS DEM with its 12.5-metre spatial resolution. This high-resolution model was instrumental in providing comprehensive topographical and hydrological data.

Table 1. Description and source of data used.

Factor	Data Source	Data format
Slope angle, slope aspect, curvature, plan curvature, profile curvature, elevation, streams, SPI, TPI, TRI, STI, FAc and TWI	Digital elevation model: Alaska Satellite Facility (ASF), ALOS, 12.5m Spatial Resolution (https://vertex.daac.asf.alaska.edu/).	Spatial raster grid data (.tif)
NDVI	Landsat-8 OLI (16 April 2023)	Spatial raster grid data (.tif)
Rainfall	General Directorate of Meteorology – Tartous Governorate	Spatial vector data (.shp)
Road	Ministry of Transport and Communications (Directorate of Transport and Public Roads – Tartous Governorate)	Spatial vector data (.shp)
Geological units and Faults	Geological maps 1/50.000 MOMR, Geology Directorate, Lattakia Governorate.	Spatial vector data (.shp)
Soil depth	Ministry of Agriculture (Directorate of Agriculture – Tartous Governorate)	Spatial vector data (.shp)
Land use/land cover	Landsat-8 OLI-TIRS, April 16, 2023 (https://earthexplorer.usgs.gov/)	Spatial raster grid data (.tif)

All factors were meticulously processed and analyzed through geographic information system (GIS) software, ensuring the data's accurate depiction and its effective application in the flood susceptibility model (Jin et al. 2023).

In addition to these factors, the study also integrated a suite of environmental variables, encompassing the Normalized Difference Vegetation Index (NDVI), rainfall patterns, road networks, geological structures, soil depth and land use/land cover (LULC) characteristics. The NDVI, sourced from the Landsat-8 OLI satellite images as of 16 April 2023, was determined by analyzing the red and near-infrared spectral bands. Stored as spatial raster grid data, it offered a precise representation of vegetative health in the region. This date was chosen for the NDVI data because it corresponds to the maximum vegetation growth period, snapshot of vegetation health and density in the study area; thus, this date has high spectral resolution potential for vegetation cover. However, providing reliable and accurate NDV data is an objective basis for completing an accurate spatial modeling of flood susceptibility using ML. LULC patterns were derived from Landsat-8 OLI-TIRS, 16 April 2023 (https://earthexplorer.usgs.gov/) to correspond to the date of conducting the current assessment. The supervised classification method was used to produce the LULC layer with a *Kappa* coefficient value of 0.88.

Rainfall information, provided in spatial vector format by the General Directorate of Meteorology of the Tartous Governorate, facilitated an understanding of regional rainfall distribution and intensity. The road data, encompassing an extensive network within the region, was supplied by the Ministry of Transport and Communications and also stored in spatial vector format. Additionally, crucial geological unit and fault line data, derived from 1:50,000 scale geological maps by the Lattakia Governorate's Geological Directorate, were pivotal in assessing the region's geological structure and potential geohazards. The soil depth data, essential for evaluating soil's influence on floodwater retention and infiltration, was provided by the Ministry of Agriculture of the Tartous Governorate, available in spatial vector format. Furthermore, the land use/land cover data, developed by ESRI and stored as spatial raster grid data, played

a significant role in analyzing the region's flood susceptibility by reflecting diverse land usage and cover types. This comprehensive data analysis lays a robust scientific groundwork, crucial for the accurate assessment of flood susceptibility in the Eastern Mediterranean region.

2.4. Flood conditioning factors

2.4.1. Slope angle

Slope angle significantly impacts both the incidence and severity of floods. Steep slopes facilitate accelerated water flow, which not only contributes to the rapid onset and movement of floods but also heightens flood risk in downstream areas. Such areas characteristically display reduced precipitation absorption, resulting in considerable surface runoff that contributes to river and lake inundation, ultimately triggering flood events. Particularly in scenarios of heavy rainfall, steep slopes are prone to soil erosion and mudslides, intensifying the destructive impact of floods and potentially leading to river blockages, which can exacerbate the extent of flood disasters.

2.4.2. Slope aspect

Slope aspect exerts a notable influence on flood dynamics due to its effects on surface water evaporation, vegetation distribution, and the snowmelt process. The slope's orientation dictates the degree of sunlight exposure, subsequently influencing the moisture content of both soil and vegetation. Sun-facing slopes, for example, are likely to experience accelerated water evaporation and drier conditions, thereby increasing the likelihood of surface runoff and subsequent flooding. Conversely, slopes that are shaded or receive less direct sunlight typically maintain higher moisture levels, which can help in mitigating runoff.

2.4.3. Curvature

The curvature of the terrain plays a pivotal role in influencing flood dynamics, particularly in terms of water direction and accumulation. Convex terrain, or positive curvature, generally results in the dispersion of water, while concave terrain, or negative curvature, tends to facilitate water accumulation. In regions with heavy rainfall, areas with concave curvature are more susceptible to waterlogging, increasing the likelihood of flooding. Plan curvature, which addresses the horizontal bending of the terrain, significantly affects both the route and velocity of water flow. Complex terrain can lead to water following a winding course, heightening the risk of localized flooding. Profile curvature, focusing on vertical terrain bending, has a direct impact on the dynamics of water flow along slopes. Slopes with a downward-facing profile curvature, leading towards rivers or lowlands, are prone to accelerated water flow downhill, thus elevating the flood risk in downstream areas. In contrast, slopes with upward-facing curvature, moving away from water bodies, can decelerate the flow of water, thereby mitigating flood risk. Consequently, understanding terrain curvature is essential in flood risk assessment and strategic land planning.

2.4.4. Elevation

The elevation of a region is a critical determinant in both the occurrence and distribution of floods. High-altitude areas often receive precipitation in the form of snow, delaying the transfer of water into the watershed system. However, during the spring thaw and periods of intense rainfall in warmer seasons, rapid melting can significantly increase water levels within the watershed, leading to floods. Conversely, lower elevation areas, particularly those with limited vegetation cover or urban development, tend to experience rapid surface runoff, primarily due to rain-based precipitation. Elevation also indirectly affects the water cycle and flood risk by influencing climatic conditions, such as temperature and evaporation rates. Higher altitudes, characterized by cooler temperatures, have slower evaporation processes, while lower altitudes may experience increased evaporation rates owing to warmer temperatures.

2.4.5. Streams

Streams are fundamental in shaping the occurrence and impact of floods. A stream's dimensions and flow rate are key determinants of its ability to manage floodwaters. Broad and deep streams have a greater capacity to contain floodwaters, thereby reducing flooding risk, whereas narrow or shallow streams are prone to overflowing during periods of heavy precipitation. The course and meandering nature of streams also plays a vital role in influencing the velocity of water flow and the spread of flood energy. Excessive meanders can cause water to accumulate, leading to localized flooding. Additionally, rainfall and snowmelt in upstream areas have a direct impact on the likelihood of flooding in downstream regions.

2.4.6. Stream Power Index (SPI)

SPI serves as an essential GIS tool to evaluate the erosive power of rivers, calculating the river's capacity for flow by integrating flow rate and slope. Rivers with elevated SPI values act as robust conduits for water and sediment transport during floods, significantly affecting the flood's trajectory, scale, and severity. In extreme weather conditions such as heavy rainfall or rapid snowmelt, regions with high SPI rivers are more susceptible to severe flooding. Consequently, the analysis of a river's SPI is vital for effective flood risk assessment and is integral to the development of early warning systems, land planning, and flood mitigation strategies. The stream power index is calculated as follows:

$$SPI = A \times \tan\beta \tag{1}$$

where A_S is the catchment area of the basin, and β is the slope angle.

2.4.7. Topographic Position Index (TPI)

TPI, another valuable GIS tool, delineates the relative height differences across terrain. This index assesses topographic position by comparing the elevation of a specific point to the elevations of its surroundings. TPI is instrumental in pinpointing areas more likely to become centers for water accumulation or dispersal. Typically, higher TPI values are associated with higher elevations, areas less prone to flooding since water naturally flows downhill (Zeng et al. 2024). In contrast, lower or negative TPI

values signify lower-lying regions, which are more vulnerable to waterlogging and an increased risk of flooding during heavy rainfall or when rivers overflow. TPI analysis, therefore, is a crucial tool in identifying low-lying areas and valleys that are prone to becoming major zones of flood accumulation and flow during severe weather conditions.

2.4.8. Terrain Ruggedness Index (TRI)

TRI, which measures the complexity of terrain, quantifies ruggedness by calculating the average variation in elevation. Higher TRI values indicate a more rugged landscape, likely to experience greater surface runoff and erosion, particularly in areas of heavy rainfall. This type of terrain limits the infiltration of water into the soil, leading to increased water flow into adjacent rivers and lakes and, consequently, a heightened potential for flooding.

2.4.9. Topographic Wetness Index (TWI)

As a GIS-based indicator, TWI evaluates the likelihood of water accumulation in specific terrain conditions. High TWI values suggest terrain that favors water retention and accumulation, contributing to higher groundwater levels and greater soil saturation. During periods of rainfall, these conditions can result in increased surface runoff, potentially triggering or intensifying flood scenarios. Thus, TWI is instrumental in enhancing our understanding and ability to predict flood risks. The calculation formula is shown in Eq. (2), where α is the upstream convergence area.

$$TWI = In(A/\tan\beta) \tag{2}$$

2.4.10. Normalized Difference Vegetation Index (NDVI)

NDVI, a pivotal remote sensing indicator, is instrumental in assessing vegetation density and health, thereby playing a significant role in understanding flood impacts. It analyzes the differential reflectance of red and near-infrared light by vegetation to provide crucial insights into vegetation coverage and growth conditions. In flood situations, regions with high NDVI values, indicative of robust vegetation cover, aid in reducing surface runoff and controlling soil erosion (Jin et al. 2023). The vegetation in these areas plays a vital role in absorbing and storing water, which contributes to slowing the water flow and reducing the risks associated with flooding. In contrast, areas characterized by low NDVI values might reflect sparse or unhealthy vegetation, heightening the risk of surface runoff and soil erosion, especially during intense rainfall events.

2.4.11. Rainfall

Rainfall is a primary and direct contributor to flood occurrences, with its volume, intensity and duration having a direct impact on the initiation and severity of floods. Heavy or prolonged rainfall can cause a swift increase in the water levels of rivers, lakes and reservoirs, leading to flooding. Variations in rainfall patterns, such as short but intense downpours, are known to provoke flash floods in urban or low-lying regions, while extended periods of rain can result in river flooding.

2.4.12. Distance to road

The distance to roads, rivers and water bodies plays a significant role in flood dynamics, primarily influencing the path of water flow and surface runoff. Roads near rivers or bodies of water can alter the natural flow of floods during heavy rainfall or rising water levels. The layout and design of road drainage systems are crucial. Well-designed road drainage systems can effectively manage surface water, mitigating flood impact even in areas close to rivers. Conversely, inadequate drainage facilities may exacerbate water accumulation in surrounding areas.

2.4.13. Geological units and faults

Geological units and faults are key players in flood occurrence and distribution, exerting their influence through regional hydrological characteristics. Different geological units, due to their varying permeability and hydrological properties, directly affect rainwater infiltration, groundwater movement, and the formation of surface runoff. Additionally, fault lines can alter the paths and speeds of groundwater flow, sometimes even acting as barriers between groundwater and surface water flow, affecting the hydrological conditions of the surrounding areas. In areas with active faults, ground movement can change the direction of surface water flow or block natural waterways, further influencing flood occurrence and distribution.

2.4.14. Soil depth

The depth of soil plays a pivotal role in influencing flood dynamics, as it directly affects the soil's capacity for water absorption and retention. Deep soils, which possess a greater ability to retain water, are more effective at absorbing rainfall. This ability not only reduces surface runoff but also significantly lowers the overall risk of flooding. Additionally, these deeper layers of soil serve as a natural buffer against floods by gradually releasing absorbed water into the groundwater system (Zhu et al. 2024). On the other hand, shallow soils, characterized by limited water retention capacity, are more likely to contribute to increased surface water flow during rain events, thereby elevating the volume of surface runoff.

2.4.15. Landuse/land cover (LULC)

The nature of land use and land cover exerts a considerable influence on flood occurrence. Urbanized or industrialized areas, characterized by extensive impermeable surfaces such as concrete and asphalt, exhibit a reduced capacity for water absorption, resulting in significant surface runoff. This runoff tends to rapidly flow to downstream areas, amplifying the risks associated with urban flooding and flash floods. In contrast, areas with natural vegetation cover, such as forests and grasslands, are more adept at absorbing rainfall. This absorption slows down the runoff process and subsequently reduces the probability of flooding. The effect of agricultural land on flooding is contingent upon specific farming practices and soil management strategies. Practices leading to soil compaction and erosion can diminish the soil's ability to absorb water, thereby increasing the likelihood and severity of surface runoff.

2.4.16. Sediment Transport Index (STI)

STI represents a pivotal measure for evaluating the ability of surface water flow to transport sediment, which significantly influences flood susceptibility. Derived from slope gradient and runoff volume, STI offers critical insights into the dynamics that contribute to the development of floods. Regions with high STI values demonstrate a greater potential for water flows to mobilize sediment, which can lead to alterations in riverbeds and channels, subsequently increasing the risk of flooding. Over time, areas characterized by elevated STI values are prone to experiencing significant changes in riverbed and channel morphology. These changes can affect the direction and velocity of river flows, impacting both the likelihood and severity of flood events. Additionally, STI bears a direct relation to ecosystem health and land use patterns. Environmental factors, such as the loss of vegetation and land development, can modify surface coverage. These alterations influence sediment transport dynamics, thereby affecting regional STI values and potentially increasing the susceptibility to flooding.

2.4.17. Flow Accumulation (FAc)

FAc measures the cumulative amount of water that converges towards a specific point, accounting for both direct precipitation and runoff from upstream sources. This metric is crucial in understanding and forecasting flood risks, as it illustrates the patterns of water accumulation and movement across landscapes. Areas with elevated FAc values are typically characterized by significant water build-up, heightening their vulnerability to floods. For example, in mountainous or hilly regions, water-descending slopes can culminate in substantial streams, often resulting in floods in lower-lying areas. In urban contexts, impermeable surfaces and heightened runoff volumes contribute to increased FAc values, thus amplifying flood risks. Moreover, FAc serves as a vital tool in identifying potential zones prone to flooding, which is indispensable for urban planning and flood management strategies. Through the analysis of FAc data, planners and managers can identify regions most susceptible to flooding. This enables the implementation of more targeted flood mitigation strategies, such as the construction of dams, detention basins, or enhanced drainage systems.

2.5. Multicollinearity test

In the assessment of flood susceptibility, the study employed the Variance Inflation Factor (VIF) and Tolerance methods to detect multicollinearity among the independent variables. Multicollinearity refers to the scenario where two or more predictors in a regression model are highly correlated, potentially leading to unreliable and unstable estimates of regression coefficients. This can compromise the predictive power and interpretability of the model. The VIF is a widely recognized metric used to quantify the severity of multicollinearity. It measures how much the variance of an estimated regression coefficient increases if predictors are correlated. A VIF value exceeding 5 (or 10 in some cases) indicates significant multicollinearity, suggesting that the predictor variables are highly correlated and may be inflating the standard errors of the regression coefficients. Conversely, Tolerance, which is the inverse of

VIF, assesses the degree of independence among the explanatory variables. A low Tolerance value suggests a higher degree of multicollinearity. It provides a direct measure of how much of the variance in a predictor can be explained by the other predictors in the model. Lower values of Tolerance (generally below 0.1) signal potential issues of multicollinearity that need to be addressed.

2.6. ML algorithms

2.6.1. Support vector machine (SVM)

SVM is a robust supervised learning algorithm predominantly used in classification and regression tasks. It functions by delineating a hyperplane that maximizes the separation margin among data points belonging to different categories. This characteristic of SVM facilitates the effective differentiation of varied data groups. In flood susceptibility assessments, the SVM model serves a critical role, analyzing a plethora of influential factors such as topography, climate conditions, and soil types to predict the probability of flooding in specific regions (Arabameri et al. 2022). Central to the SVM approach is the creation of an optimal decision boundary, designed to maximize the distance between different data point categories. The model's capability to manage nonlinear relationships is enhanced by its use of suitable kernel functions (Akhter et al. 2025). This adaptability renders it highly effective for intricate analyses involved in flood susceptibility studies. Depending on the unique attributes of the dataset and specific problem requirements, a range of kernel functions, like linear, polynomial, or Radial Basis Function (RBF), can be utilized.

2.6.2. Random forest (RF)

RF algorithm is integral to flood susceptibility assessment research. This ensemble learning method boosts prediction accuracy by building and integrating multiple decision trees. Each tree is trained on a distinct set of data samples and features, culminating in a combined prediction that synthesizes the individual trees' outputs. This methodology notably curtails the risk of overfitting specific data sets, thus enhancing the model's applicability to a wide array of data. In tackling the intricate challenges of flood susceptibility assessment, random forest showcases its distinct advantages (Avand et al. 2022). Capable of handling multifaceted data, including terrain features, climatic variables, soil characteristics, and vegetation patterns, it offers a holistic evaluation of factors contributing to flood risk (Sharma et al. 2024). By delving into such a varied data spectrum, RF adeptly forecasts potential flood occurrences in targeted areas and pinpoints critical determinants of flood risk.

2.6.3. Artificial neural network (ANN)

ANN model is crucial in assessing flood susceptibility. This computational model, mimicking the human brain's neural network, consists of a complex array of interconnected nodes across various layers, including the input, hidden, and output layers. ANN's main advantage lies in its exceptional nonlinear modeling capabilities, equipping it to address the intricate nonlinear relationships that are often pivotal in flood susceptibility assessments. Moreover, ANN is distinguished by its adaptability and flexibility, boasting self-

learning abilities that enable it to discern and adapt to key data features, thus enhancing its efficiency in handling complex datasets. The model's robust generalization skills are particularly noteworthy, as they facilitate accurate predictions about unfamiliar data, a key component in predicting future flood-prone zones. Additionally, ANN's capacity to process a vast range of data inputs, encompassing elements like topography, climatic conditions, soil characteristics and human activities, significantly augments the thoroughness and accuracy of flood susceptibility evaluations. Consequently, ANN presents itself as an effective, versatile and precise tool in the prediction of flood risks. Its strong computational prowess and reliable outputs offer substantial technical support in the formulation and implementation of flood prevention and mitigation strategies, thereby contributing significantly to the field of flood risk management.

2.6.4. Extreme Gradient Boost (XGBoost)

Extreme Gradient Boosting, commonly known as XGBoost, stands as a highly efficient and potent algorithm within the field of ML (Zeng et al. 2023). Functioning as an ensemble learning algorithm, XGBoost leverages decision trees to enhance the precision and efficiency of predictions. This is achieved by constructing and integrating a series of decision trees, thereby amplifying the overall predictive strength. At its core, XGBoost operates on the principle of the gradient boosting framework (Salem et al. 2025). This involves a sequential building process, where each iteration contributes to a new decision tree. These trees are designed to adjust and improve upon the predictions made by their predecessors, aiming for a progressive alignment with actual values. The construction of each subsequent tree is focused on reducing the residuals left by the previous iteration, ultimately striving to minimize the total predictive error of the model (Zhu et al. 2024). Among the notable strengths of XGBoost are its exceptional computational speed and outstanding predictive accuracy. It is equipped with parallel processing capabilities, markedly enhancing the construction efficiency of decision trees. Moreover, XGBoost addresses the challenge of overfitting by integrating regularization terms. This feature helps in managing the model's complexity, thereby curtailing the likelihood of overfitting. Additionally, XGBoost's versatility allows it to manage missing values and support various objective functions, making it adept at handling diverse and complex data scenarios. With its robust data processing abilities and precision in predictions, XGBoost has become an essential asset in the assessment of flood susceptibility, offering valuable insights and predictions in this critical area of study.

2.7. Performance assessment of applied algorithms

In this assessment, several statistical criteria, including precision, recall, F1 score, accuracy and ROC-AUC (Eqs. (3)–(8)), have been implemented to assess the efficiency and reliability of the used models. All these metrics are calculated using the values of different possible consequences (PC), namely false positive (FP), false negative (FN), true positive (TP), and true negative (TN). In the case of FP and FN, these wrongly classify the pixels of flood and non-flood, while TP and TN correctly classify the flood and non-flood locations. The applied statistical measures are determined based on Eqs. (3)–(8).

$$Recall/Sensitivity = \frac{TP}{TP + FN} \tag{3}$$

$$Specificity = \frac{TN}{TN + FP} \tag{4}$$

$$Precision = \frac{TP}{TP + FP} \tag{5}$$

$$F1 = \frac{2TP}{2TP + FP + FN} \tag{6}$$

$$Accuracy = \frac{TP + TN}{TP + TN + FP + FN} \tag{7}$$

In evaluating flood susceptibility, the Area Under the Receiver Operating Characteristic Curve (ROC AUC) was employed as a key measure to gauge the performance of our models. The ROC curve, a graphical representation, illustrates the performance of classification models over an array of possible thresholds. The AUC value, delineated by the area beneath this curve, is an essential indicator of a model's capability to classify accurately. Spanning from 0 to 1, higher AUC values denote enhanced classification efficacy of the model. Specifically in flood susceptibility assessment, a substantial AUC value signifies the model's proficiency in effectively differentiating flood-prone areas from those less susceptible, thus enabling precise predictions about flood likelihood. Consequently, the ROC curve and its associated AUC value offer a straightforward and efficacious approach to validate and benchmark the performance of various models in their capacity to forecast flood susceptibility.

$$AUC = \sum TP + \sum TN/(K + S) \tag{8}$$

where K denotes total number of flood events and S represents the total number of flood events.

To perform an analysis of the existence of statistically significant variation or not between the performances of the four models, the Friedman test was conducted. The Friedman non-parametric test is given by Eq. (9). However, p value < 0.05 is assessed significant, and vice versa.

$$F_r = \frac{12}{nk(k+1)} \sum_{i=1}^{k} R_i^2 - 3(k+1) \tag{9}$$

where $n =$ number of density fractions, and $k =$ number of samples.

3. Results

3.1. Multicollinearity investigation of flood causative factors

The selection of significant flood-influencing variables is the primary step in flood susceptibility mapping. Relevant variables enhance the precision of ML models by eliminating insignificant factors (Prasad et al. 2022). In the present research, twenty geo-environmental factors have been taken to select the relevant factors for training the ML models. Therefore, multicollinearity analysis used variance inflation factors and tolerance methods to assess the correlation among the causative factors. Values greater than 10 for VIF and less than 0.1 for tolerance indicate multicollinearity. Based on the multicollinearity results, no serious collinearity has been found among the conditioning variables (Table 2). Although SPI has the highest VIF (7.54) and the lowest TOL (0.13) values, it has not exceeded the theoretical threshold values. Since all the flood-affecting variables are within a range of the theoretical values, it has been decided to incorporate all factors for analysis.

3.2. Flood causative factor analysis

In this study, twenty flood conditioning variables, including rainfall, elevation, slope degree, aspect, curvature, profile curvature, plan curvature, NDVI, LULC, SPI, TWI, TPI, lithology, distance to faults, distance to river, distance to road, soil depth, TRI, STI, and flow accumulation, have been considered for modelling. Various aspects of rainfall, like duration, intensity, amount, and distribution, are crucial factors for flash floods in an area (Prasad et al. 2022). The distribution of rainfall is diversified from 847 to 1359 mm from east to west of the study region (Figure 2(a)). The elevation of the region varies from 24 to 911 m above mean sea level (Figure 2(b)). The higher range of elevation (887 m) influences the slope value from 0 to 53 degrees (Figure 2(c)). Aspect map has been classified into ten different slope directions, namely flat,

Table 2. Multicollinearity test results for flood causative factors.

Causative factors	VIF	TOL
Rainfall	1.302	0.77
Elevation	1.552	0.64
Slope degree	1.840	0.54
Aspect	1.205	0.83
Curvature	1.097	0.91
Profile Curvature	2.218	0.45
Plan Curvature	1.642	0.61
NDVI	1.882	0.53
LULC	1.320	0.76
SPI	7.541	0.13
TWI	1.700	0.59
TPI	3.496	0.29
Lithology	1.453	0.69
Distance to faults	1.160	0.86
Distance to river	2.547	0.39
Distance to road	1.183	0.85
Soil depth	1.473	0.68
TRI	1.513	0.66
STI	4.134	0.24
Flow accumulation	3.480	0.29

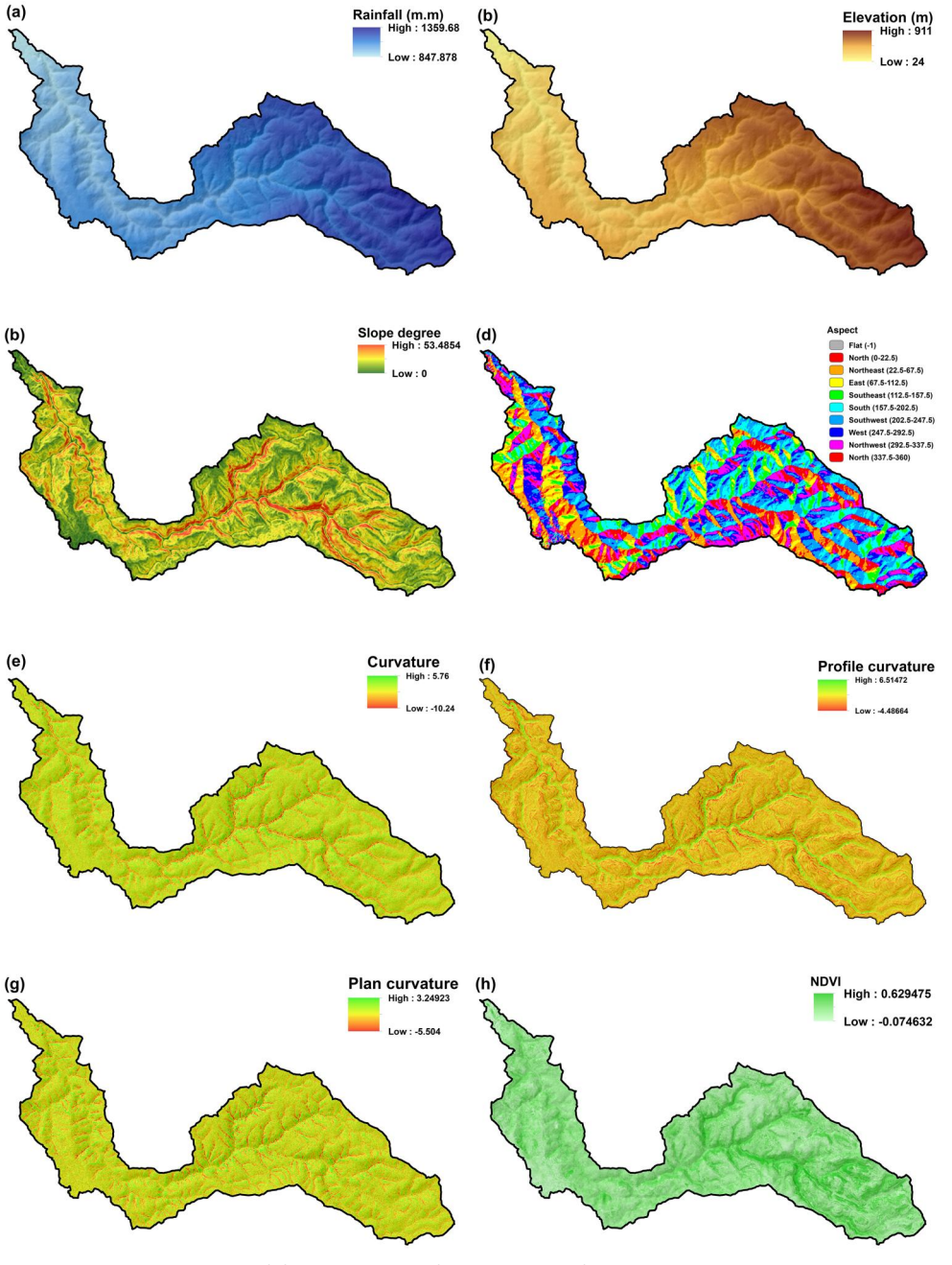

Figure 2. Thematic layers of flood causative factors: (a) rainfall, (b) elevation, (c) slope angels, (d) slope aspect, (e) curvature, (f), profile curvature, (g) plan curvature, (h) NDVI, (i) LULC, (j) SPI, (k) TWI, (l) TPI, (m) lithology, (n) distance to faults, (o) distance to Rivers, (p) distance to roads,(q) soil depth, (r) TRI, (s) STI, (t) flow accumulation.

north, northeast, east, southeast, south, southwest, west, northwest and north (Figure 2(d)). Curvature maps, including standard curvature, plan curvature and standard curvature, are shown in Figure 2(e)–(g), respectively. Positive profile curvature values

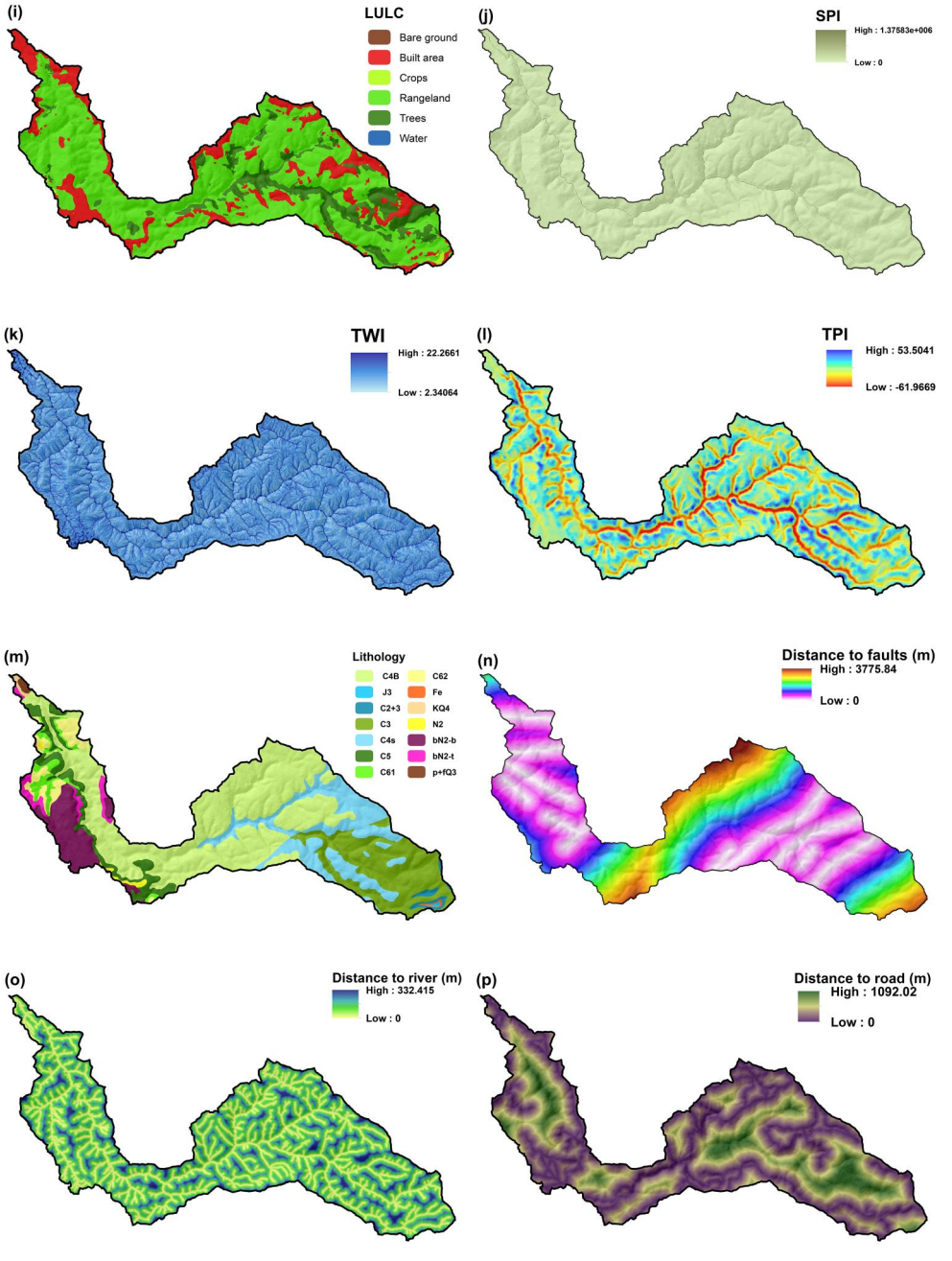

Figure 2. Continued.

indicate an upwardly concave surface, while negative values represent an upwardly convex surface. On the other hand, positive and negative values of planform curvature are exhibited on the sideward convex and sideward concave surfaces, respectively. The NDVI values differ from −0.07 to 0.62 (Figure 2(h)). LULC of the region is divided into six different categories: bare ground, built-up, crops, rangeland, forest and water bodies (Figure 2(i)). The SPI values are relatively low, which is also

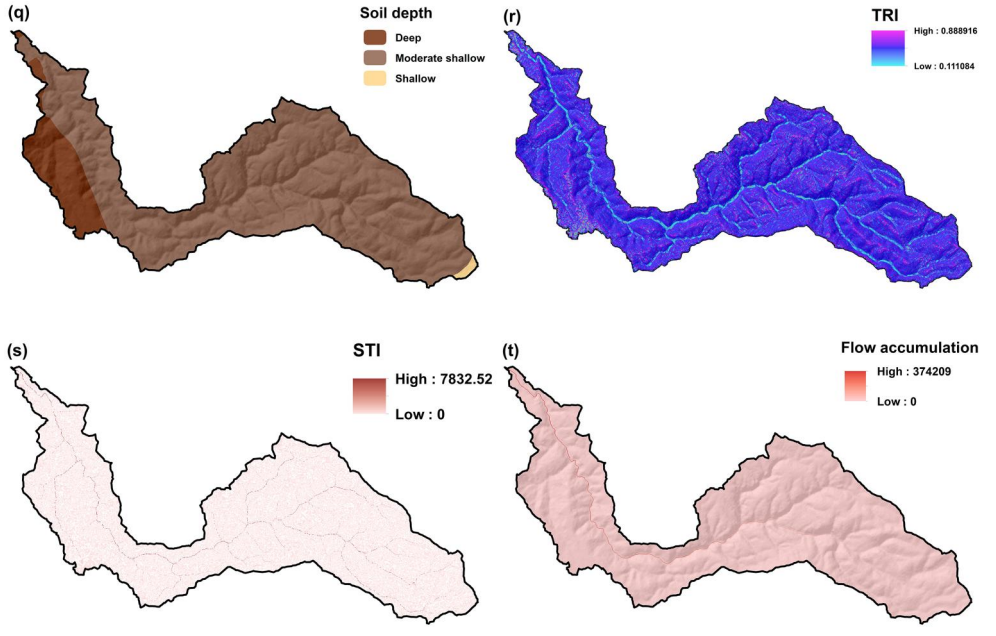

Figure 2. Continued.

reflected in high VIF and low tolerance values (Figure 2(j)). TWI values range between 2 and 22, indicating high wetness in the region (Figure 2(k)). TPI values span a wide range, starting from −61 and ending at +51 (Figure 2(l)). The obtained lithology map has been classified into fourteen different lithological units, namely upper part of Cenomanian (C4B), upper part of Cenomanian (C4S), Albian (C3), Aptian and Lower Albian (C2 + 3), Upper Jurassic (J3), limonitic iron ore (Fe), Turonian limestone (C5), Maastrichtian (C62), Coniacian-Santonian (C61), Pliocene basalt-tuff lava (N2), Pliocene basalt (βN2-b), Pliocene tuff (βN2-t), Holocene Kolluvium (KQ4) and Upper Pleistocene boulders, Gravel and sand (P + fQ3) (Figure 2(m)). From Figure 2(n), it is observed that the distance from the fault to flood occurrence locations is greater in the middle portion, while eastern and western regions (except some portions of the west) have a lower density of faults. The distance to rivers and roads for flood events varies up to 332 m and 1,092 m, respectively (Figures 2(o) and (p)). Soil depth in the study region is divided into three horizons: deep, moderately shallow and shallow (Figure 2(q)). The topographical roughness values fall between 0.11 and 0.88 (Figure 2(r)). In the case of STI, it ranges from 0 to 7,832 (Figure 2(s)). Flow accumulation achieves the highest pixel value of 37,4209 (Figure 2(t)).

3.3. Importance of causative factors

The role of each flood-conditioning factor varies across the world due to different geo-environmental conditions. Therefore, it is necessary to understand the importance of flood-influencing variables to comprehend the role of each factor in the occurrence of floods in a specific area of interest. Following multicollinearity analysis,

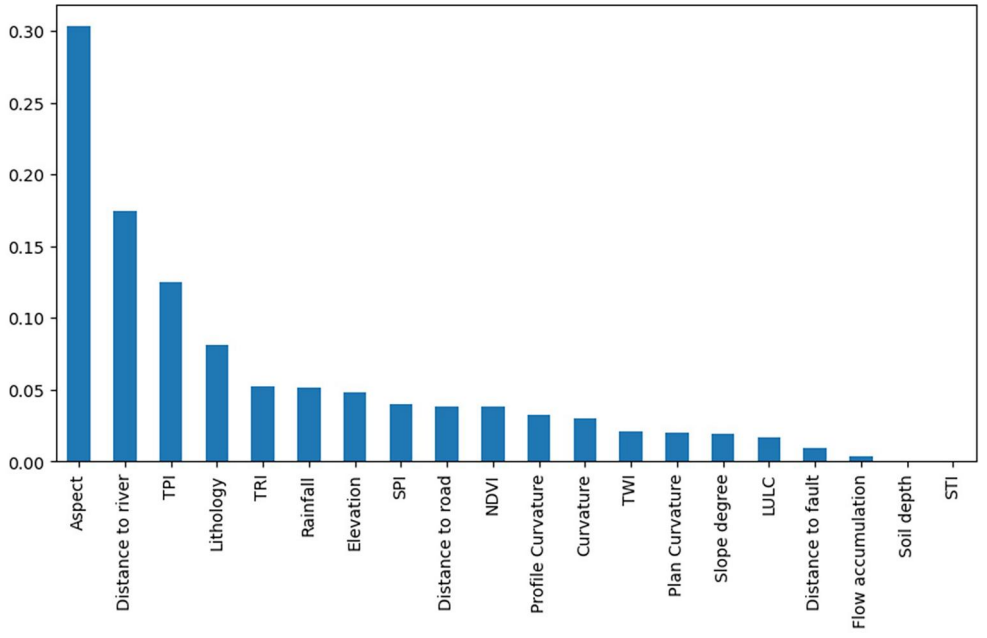

Figure 3. Importance of flood susceptibility causative factors.

20 flood-conditioning factors have been selected for this study, and their importance is illustrated in Figure 3. The results showed that the most important variable is aspect, followed by distance to river, TPI and lithology. In contrast, the least important variables are STI, soil depth, flow accumulation and distance to fault. The categorical variable LULC does not exert a significant influence on flood occurrence in the study region. The highest contribution of the aspect factor in the current study is also reflected in the research of Yariyan et al. (2020). The high contribution of the aspect factor in this study aligns with the findings of Yariyan et al. (2020). Similarly, in the study by Pham et al. (2020), the role of distance to the river in flood events is emphasized compared to other flood conditioning factors in the Markazi province in Iran.

3.4. Flood susceptibility maps

Many studies have been done for flood susceptibility mapping across the world using different statistical, ML and deep learning methods (Yariyan et al. 2020). However, there is no universally accepted model used for flood zonation due to the heterogeneous characteristics of the earth. For this, in the current research, four popular ML models, including RF, XGBoost, SVM and ANN, have been employed to compare the model precisions and prepare the flood susceptibility maps for the study area.

The selection of these ML models for flood susceptibility mapping in this assessment is justified by their ability to handle complex, high-dimensional data and capture non-linear relationships. RF and XGBoost offer robustness against overfitting and provide insights into feature importance, which is crucial for understanding flood drivers. SVM balances nonlinear modeling with interpretability, while ANN excels in

Table 3. Optimization of ML models.

model	Hyper_parameter	Optimal value
XGB	n_estimators	200
	learning_rate	0.5
	max_depth	7
RF	n_estimators	50
	min_samples_split	5
	max_features	log2
	max_depth	15
SVM	kernel	rbf
	probability	True
	C	1
	gamma	auto
ANN	activation	tanh
	optimizer	adam
	epochs	90
	Batch_size	10

capturing intricate patterns. Additionally, these models are computationally efficient and have established track records in similar environmental studies, making them suitable for this analysis.

The susceptibility map is prepared based on the predicted probability values of the models. Regions with higher probability values indicate greater vulnerability to floods, while those with lower values are less prone to floods. In many studies, probability values are classified using different methods, namely geometrical, standard deviation, equal interval, natural break, min-max normalization, and quantile, to illustrate the intensity of flood occurrence (Pham et al. 2020). In this regard, the process of optimizing the ML algorithm models used is a fundamental step in this analysis. The GridSearch CV process was used to identify the optimal parameters or optimize the hyperparameters tuning parameters of each model (Table 3).

According to the nature of the model's output, the natural break method has been employed in this research to generate flood susceptibility maps. These maps are classified using *Natural Breaks* method into five zones: very high, high, moderate, low and very low (Figure 4(a)–(d)). The real distributions of flood-susceptible classes from different models are presented in Table 4. It is observed that the combined high and very high classes cover 37.8%, 40.8%, 41.4% and 36.7% of the total study region for RF, XGBoost, SVM and ANN models, respectively. The low variation (<5%) in spatial coverage demonstrates the precision of the model's classification. From the flood susceptibility maps, it is observed that the eastern part of the study region is more exposed to floods compared to the western region. Additionally, areas near rivers and confluence zones of streams are more vulnerable to floods, consistent with findings in several studies (Janizadeh et al. 2019; Prasad et al. 2022). Overall, approximately 35% of the study region is susceptible to flood hazards, suggesting the need for monitoring and planning.

3.5. Model validation

Model validation is the final and crucial step in ML to comprehend and evaluate different methods (Prasad et al. 2022). In this study, the applied ML models have been

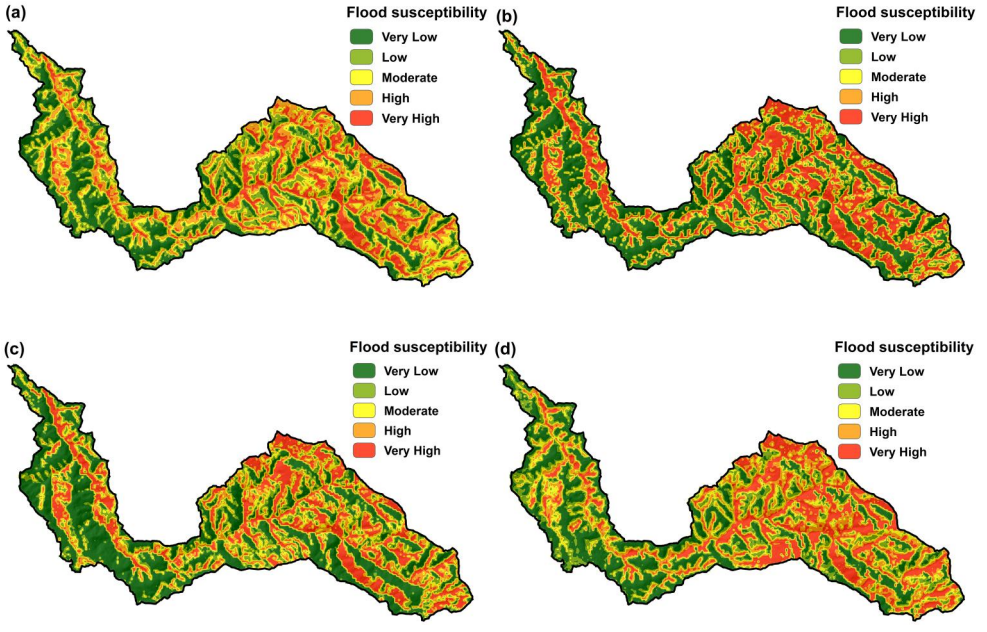

Figure 4. Flood susceptibility maps (a) RF, (b) XGBoost, (c) SVM and (d) ANN.

Table 4. Areal distributions of flood-susceptible classes from different models.

	RF		XGBoost		SVM		ANN	
Class	KM^2	%	KM^2	%	KM^2	%	KM^2	%
Very low	16.49	**28.18**%	26.88	**45.92**%	18.35	**31.33**%	24.97	**42.66**%
Low	10.40	**17.77**%	4.45	**7.60**%	8.83	**15.08**%	6.52	**11.15**%
Moderate	9.53	**16.28**%	3.33	**5.69**%	7.15	**12.21**%	5.58	**9.54**%
High	11.10	**18.97**%	4.22	**7.22**%	8.73	**14.92**%	6.60	**11.29**%
Very high	10.99	**18.79**%	19.64	**33.56**%	15.49	**26.46**%	14.84	**25.36**%

Table 5. Precision indices of different used models.

Classifier	Precision	Recall	F1 score	Accuracy	AUC
RF	0.91	0.95	0.93	0.93	0.98
XGBoost	0.93	0.95	0.94	0.94	0.98
SVM	0.87	0.93	0.9	0.9	0.94
ANN	0.92	0.91	0.92	0.92	0.97

trained using the 10-fold cross-validation method to avoid the overfitting problem. These models have been evaluated using a set of quantitative criteria, namely precision, recall, F1 score, accuracy and AUC. Table 5 presents the statistical indices of different models to compare their precision.

The testing dataset (30%) has been used to evaluate and compare the models because it showcases the predictive power of the model (Prasad et al. 2022). In terms of precision, the XGBoost model (0.93) demonstrated superiority, followed by ANN (0.92), RF (0.91) and SVM (0.87). The RF and XGBoost models obtained the same recall value (0.95), while SVM achieved 0.93 and ANN received 0.91. Regarding F1 score and accuracy, XGBoost, RF, ANN and SVM models achieved 0.94, 0.93, 0.92

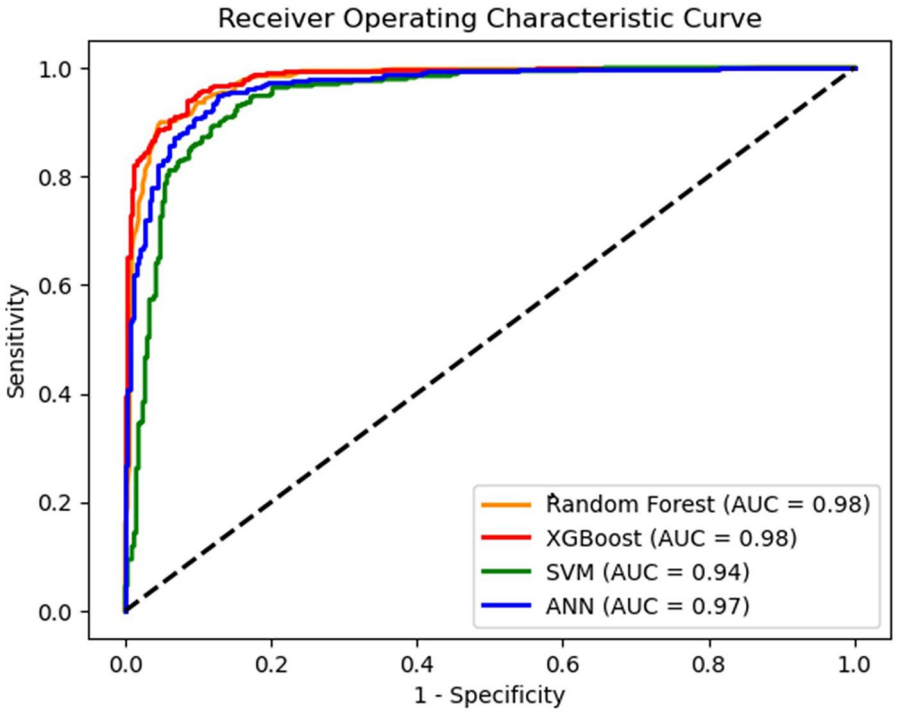

Figure 5. ROC curve for implemented ML models.

Table 6. Friedman test results.

	Mean ranks	Chi-square	*p* value
RF	1.60	26.08	0.00001
SVM	3.20		
ANN	3.80		
XGB	1.40		

and 0.9, respectively. Hence, most of the researchers considered that the ROC-AUC method is effective in evaluating the efficiency of the models.

The AUC values of the models in descending order are 0.98 (XGBoost), 0.98 (RF), 0.97 (ANN) and 0.94 (SVM) as Figure 5 illustrates. Based on all the quantitative criteria, it is evident that the XGBoost model achieved the highest accuracy, followed by RF, ANN and SVM. Nevertheless, all the models have obtained more than 90% accuracy, making them suitable for preparing the flood susceptibility map of the study region. Referring to the *p* value, which is lower than 0.05 for all ML algorithms in the Friedman test result (Table 6), indicates a statistically significant contrast in performance among the ML models.

4. Discussion

The Eastern Mediterranean region is vulnerable to frequent flood events, causing severe human and economic losses. Flood susceptibility maps are one of the most important basics of comprehensive land management of this imminent risk.

Continuous improvement of the quality of flood susceptibility maps is an urgent need. This study presented an objective investigation into evaluating the performance of four ML algorithms in mapping flood susceptibility in the Eastern Mediterranean towards more accurate modeling.

Assessing flood susceptibility maps to accurately spot flood-prone areas is one of the most essential preventive measures in flood disaster risk reduction and management. Therefore, advanced modelling methods are highly encouraged to explore or apply for mapping flood-prone areas (Seydi et al. 2022). Furthermore, the regions where flood control measurements must be collected primarily for effective and efficient flood management have been identified using effective integration between ML algorithms and geospatial tools. Hence, the eastern region in the basin which is identified to be highly susceptible to floods should be assessed as part of the two common management strategies, protection and recovery, respectively.

The flood susceptibility maps derived from SVM, RF, ANN and XGBoost models have indicated that the eastern part of the study region is more vulnerable to flooding than the western region. The eastern region is dominantly characterized by southeast and south aspects, high distance to river and high TPI. Moreover, the findings that near river locations and confluence zones of streams are more vulnerable to floods, aligned with the published scholars (Janizadeh et al. 2019; Prasad et al. 2022).

In general, flood events are associated with the amount and severity of the precipitation. However, all other factors, such as elevation, slope, distance to river, LULC and soil, should be considered when determining the flood susceptibility of a basin. It can be observed that the importance of influencing factors was identified differently depending on the algorithms and characteristics of the study sites. For instance, an increase in altitude and slope angle would increase rainfall; however, that increase in precipitation intensity may not influence flood events at lower altitudes and slopes (Hadian et al. 2022). Among influencing factors, morphological properties may significantly estimate the flood vulnerability in the Mediterranean basin, considering its sparse vegetation and shallow soils. This is reflected by the findings in this study, where aspect, distance to river and TPI are the most important factors influencing flood susceptibility assessment, compared to LULC and soil depth, which ranked among the lowest.

Moreover, other environmental and human factors, including LULC, soil type and urban development, have a significant impact on the risk of floods. The LULC patterns in the Banias River basin are undergoing rapid change under the influence of population growth, especially the loss of vegetation cover and urban expansion, thus enhancing the devastating effects of floods. Urban development in the study area, especially urban expansion, increases the impermeable land cover. This expansion is also random with the absence of efficient drainage systems. As for the soil type, clayey soils predominate along the river courses in the study area. The clayey texture has a positive effect in increasing the impact of flood events.

ML algorithms are a powerful tool for determining flood susceptibility, which often involves dealing with high-dimensional and complex interactions among various environmental and geographical features. ML models, such as RF, ANN and XGBoost, in particular, offer insights into feature importance, enabling the identification of key

variables influencing flood susceptibility. In addition, ML models exhibit robustness to outliers, an important characteristic when dealing with environmental data that often includes extreme events. These strengths of ML algorithms provide reliable models with high predictive accuracy for assessing flood susceptibility. Furthermore, ensemble ML algorithms, such as RF, potentially generate better performance compared to others. For example, Özdemir et al. (2023) reported that ML models coupled with preprocessing and hyperparameter optimization produce more successfully modeled flood susceptibility areas in the Eastern Mediterranean basin. This is in agreement with the findings from this study, where the two ML models, XGBoost and RF, are superior to SVM and ANN models.

The Eastern Mediterranean basin, together with the Asi and Ceyhan basins, showed the largest changes in the future forecasts of the annual total precipitation (Özdemir et al. 2023). It is reported that although precipitation has generally decreased in the Eastern Mediterranean basin, recent years have shown that short, powerful bursts of rainfall, particularly in highly populated regions near the shoreline, which can cause flash floods due to rising temperatures and evaporation. In addition, it is expected that as a result of climate change-induced extreme rainfall events, flood events will occur more frequently and with greater intensity. Climate change projections list the Mediterranean region as one of the hotspots. Thus, the Eastern Mediterranean basin was selected for this study and others (Özdemir et al. 2023) due to the heavily populated coastal areas that are vulnerable to flash floods and the growing impact of climate change on these natural disasters. The flood susceptibility maps produced from this study can assist national, regional and local response agencies in making better-informed decisions by enabling effective flood management plans for the basin. Future research may also account for human activities that disrupt hydrologic systems to produce more accurate results. Furthermore, several challenges, such as interpretability, sensitivity to parameter tuning, overfitting and computational resources, may need to be taken into account when applying ML models for flood susceptibility tasks.

5. Conclusions

Accurate and reliable flood susceptibility mapping is considered a crucial measure in strategically managing devastating flood consequences in the Eastern Mediterranean. In this study, the performance of four ML algorithms, that is XGBoost, RF, SVM and ANN models, in mapping flood susceptibility for the first time in Syria was evaluated and tested for the first time. This investigation identified a total of 1,100 flood events in the Baniyas River Basin, western Syria, with twenty influencing factors. The suitability of these factors to the modeling process was measured using a multicollinearity test, which emphasized the importance of all factors. The quality of the produced maps was tested using several accuracy assessment indicators, including the ROC curve. The results showed that all the applied algorithms achieved high and reliable accuracy. Hence, both RF and XGBoost algorithms achieved the highest accuracy compared to the rest of the algorithms with an AUC value of 0.98. Moreover, it was found that about 30% of

the study area is vulnerable to high flood hazards. These high-risk areas are concentrated along river courses, especially in the central and southwestern parts. The process of flood susceptibility modelling is a critical and complex procedure, especially in data-scarce areas. However, the use of ML algorithms has enabled the improvement of flood susceptibility maps in Syria, which suffers from the consequences of war, especially in the field of watershed management. Overall, the current results represent an important basis for decision-makers and land use planners to determine the spatial distribution of potential flood risk and thus better spatial management of lands in western Syria.

One of the limitations of this study was the difficulty of obtaining the necessary data, especially the data on the driving factors. The field work was also hampered at some stages during the completion of this study. However, objective alternatives and sufficient facilities were found to complete this study. This study recommends expanding the assessments to the rest of the river basins in the Eastern Mediterranean, in addition to the need for continuous improvement of machine learning algorithms to ensure the highest possible accuracy of flood susceptibility maps.

In this regard, the resulting flood maps have a crucial role for decision-makers and managers of the study basin in determining priorities for infrastructure investments, especially in the field of surface runoff management. For example, building dams, establishing modern drainage systems, and building emergency and rapid response systems. The current results also provide informed insights for planners, especially in the field of community management and enhancing the community's ability to face potential flood risks. Providing community participation, safe land use planning, neutralizing high-risk areas, and community awareness are among the most important strategies recommended for policy-makers to manage flood risks in a country that suffers a lot like Syria.

Acknowledgment

The authors extend their appreciation to the Deanship of Scientific Research at King Khalid University for funding this work through Research Group under grant number RGP2/412/45.

Author contributions

CRediT: **Hazem Ghassan Abdo**: Conceptualization, Supervision, Writing – review & editing; **Sahar Mohammed Richi**: Data curation, Formal analysis, Investigation, Validation, Visualization; **Taorui Zeng**: Methodology, Writing – original draft; **Saeed Alqadhi**: Formal analysis, Resources, Writing – original draft; **Pankaj Prasad**: Software, Writing – original draft, Writing – review & editing; **Thong Nguyen-Huy**: Writing – original draft; **Maged Muteb Alharbi**: Investigation, Writing – original draft; **Javed Mallick**: Writing – original draft, Writing – review & editing.

Disclosure statement

The authors declare that they have no known competing financial interests or personal relationships that could have appeared to influence the work reported in this paper.

Funding

The authors extend their appreciation to the Deanship of Scientific Research at King Khalid University for funding this work through Large Groups Project under grant number RGP 2/412/45.

ORCID

Hazem Ghassan Abdo http://orcid.org/0000-0001-9283-3947
Sahar Mohammed Richi http://orcid.org/0009-0008-3409-8815

Availability of data

The data that support the findings of this study are available on request from the corresponding author.

References

Abd-Elhamid HF, Zeleňáková M, Soľáková T, Saleh OK, El-Dakak AM. 2024. Monitoring flood and drought risks in arid and semi-arid regions using remote sensing data and standardized precipitation index: a case study of Syria. J Flood Risk Management. 17(1):e12961. doi: 10.1111/jfr3.12961.

Abdo HG. 2020. Evolving a total-evaluation map of flash flood hazard for hydro-prioritization based on geohydromorphometric parameters and GIS–RS manner in Al-Hussain river basin, Tartous, Syria. Nat Hazards. 104(1):681–703. doi: 10.1007/s11069-020-04186-3.

Akhter S, Rahman MM, Monir MM. 2025. Flood susceptibility analysis to sustainable development using MCDA and support vector machine models by GIS in the selected area of the Teesta River floodplain, Bangladesh. HydroResearch. 8:127–138. doi: 10.1016/j.hydres.2024.10.004.

Alogayell HM, Kamal A, Alkadi II, Ramadan MS, Ramadan RH, Zeidan AM. 2024. Spatial modeling of land resources and constraints to guide urban development in Saudi Arabia's NEOM region using geomatics techniques. Front Sustain Cities. 6:1370881. doi: 10.3389/frsc.2024.1370881.

Alrawi I, Chen J, Othman AA, Ali SS, Harash F. 2023. Insights of dam site selection for rainwater harvesting using GIS: a case study in the Al-Qalamoun Basin, Syria. Heliyon. 9(9):e19795. doi: 10.1016/j.heliyon.2023.e19795.

Al-Ruzouq R, Shanableh A, Jena R, Gibril MBA, Hammouri NA, Lamghari F. 2024. Flood susceptibility mapping using a novel integration of multi-temporal sentinel-1 data and eXtreme deep learning model. G. Front. 15(3):101780. doi: 10.1016/j.gsf.2024.101780.

Alsafadi K, Mohammed S, Mokhtar A, Sharaf M, He H. 2021. Fine-resolution precipitation mapping over Syria using local regression and spatial interpolation. Atmos Res. 256:105524. doi: 10.1016/j.atmosres.2021.105524.

Alzubaidi L, Zhang J, Humaidi AJ, Al-Dujaili A, Duan Y, Al-Shamma O, Santamaría J, Fadhel MA, Al-Amidie M, Farhan L. 2021. Review of deep learning: concepts, CNN architectures, challenges, applications, future directions. J Big Data. 8(1):53. doi: 10.1186/s40537-021-00444-8.

Arabameri A, Seyed Danesh A, Santosh M, Cerda A, Chandra Pal S, Ghorbanzadeh O, Roy P, Chowdhuri I. 2022. Flood susceptibility mapping using meta-heuristic algorithms. Geomatics Nat Hazards Risk. 13(1):949–974. doi: 10.1080/19475705.2022.2060138.

Avand M, Kuriqi A, Khazaei M, Ghorbanzadeh O. 2022. DEM resolution effects on machine learning performance for flood probability mapping. J Hydro-Environ Res. 40:1–16. doi: 10.1016/j.jher.2021.10.002.

Badreldin H, Scaini C, Hassan HM, Peresan A. 2025. High-resolution multi-hazard residential buildings and population exposure model for coastal areas: A case study in northeastern Italy. Int. J. Disaster Risk Reduct. 121:105403 10.1016/j.ijdrr.2025.105403.

Costache R, Arabameri A, Elkhrachy I, Ghorbanzadeh O, Pham QB. 2021. Detection of areas prone to flood risk using state-of-the-art machine learning models. Geomatics Nat. Hazards Risk. 12(1):1488–1507. doi: 10.1080/19475705.2021.1920480.

Dawson M, Lewin J. 2024. The heterogeneous geomorphological impact of an exceptional flood event and the role of floodplain vegetation. Earth Surf Processes Landf. 49(1):354–373. doi: 10.1002/esp.5707.

Dutta M, Saha S, Saikh NI, Sarkar D, Mondal P. 2023. Application of bivariate approaches for flood susceptibility mapping: a district level study in Eastern India. HydroResearch. 6:108–121. doi: 10.1016/j.hydres.2023.02.004.

El-Aal AA, Radwan AE, Abdelshafy M, Omaar AE, Youssef YM. 2024. A synergistic use of remote sensing and hydrodynamic techniques for flash flood mitigation toward sustainable urban expansion in Najran Valley, Saudi Arabia. Earth Syst Environ. 8(2):465–482. doi: 10.1007/s41748-024-00371-7.

Essam Y, Huang YF, Ng JL, Birima AH, Ahmed AN, El-Shafie A. 2022. Predicting streamflow in Peninsular Malaysia using support vector machine and deep learning algorithms. Sci Rep. 12(1):3883. doi: 10.1038/s41598-022-07693-4.

Farhadi H, Esmaeily A, Najafzadeh M. 2022. Flood monitoring by integration of Remote Sensing technique and Multi-Criteria Decision Making method. Comput Geosci. 160:105045. doi: 10.1016/j.cageo.2022.105045.

Hadian S, Shahiri Tabarestani E, Pham QB. 2022. Multi Attributive Ideal-Real Comparative Analysis (MAIRCA) method for evaluating flood susceptibility in a temperate Mediterranean climate. Hydrol Sci J. 67(3):401–418. doi: 10.1080/02626667.2022.2027949.

He F, Liu S, Mo X, Wang Z. 2025. Interpretable flash flood susceptibility mapping in Yarlung Tsangpo River Basin using H2O Auto-ML. Sci Rep. 15(1):1702. doi: 10.1038/s41598-024-84655-y.

Janizadeh S, Avand M, Jaafari A, Phong TV, Bayat M, Ahmadisharaf E, Prakash I, Pham BT, Lee S. 2019. Prediction success of machine learning methods for flash flood susceptibility mapping in the Tafresh Watershed, Iran. Sustainability. 11(19):5426. doi: 10.3390/su11195426.

Jin B, Zeng T, Yang T, Gui L, Yin K, Guo B, Zhao B, Li Q. 2023. The prediction of transmission towers' foundation ground subsidence in the salt lake area based on multi-temporal interferometric synthetic aperture radar and deep learning. Remote Sens. 15(19):4805. doi: 10.3390/rs15194805.

Kalantar B, Ueda N, Saeidi V, Janizadeh S, Shabani F, Ahmadi K, Shabani F. 2021. Deep neural network utilizing remote sensing datasets for flood hazard susceptibility mapping in Brisbane, Australia. Remote Sens. 13(13):2638. doi: 10.3390/rs13132638.

Nachappa TG, Piralilou ST, Gholamnia K, Ghorbanzadeh O, Rahmati O, Blaschke T. 2020. Flood susceptibility mapping with machine learning, multi-criteria decision analysis and ensemble using Dempster Shafer Theory. J. Hydrol. 590:125275. doi: 10.1016/j.jhydrol.2020.125275.

Özdemir H, Baduna Koçyiğit M, Akay D. 2023. Flood susceptibility mapping with ensemble machine learning: a case of Eastern Mediterranean basin, Türkiye. Stoch Environ Res Risk Assess. 37(11):4273–4290. doi: 10.1007/s00477-023-02507-z.

Peresan A, Hassan HM. 2024. Scenario-based tsunami hazard assessment for Northeastern Adriatic coasts. Med Geosc Rev. 6(2):87–110. 10.1007/s42990-024-00114-w.

Pham BT, Avand M, Janizadeh S, Phong TV, Al-Ansari N, Ho LS, Das S, Le HV, Amini A, Bozchaloei SK, et al. 2020. GIS based hybrid computational approaches for flash flood susceptibility assessment. Water. 12(3):683. doi: 10.3390/w12030683.

Prasad P, Loveson VJ, Das B, Kotha M. 2022. Novel ensemble machine learning models in flood susceptibility mapping. Geocarto Int. 37(16):4571–4593. doi: 10.1080/10106049.2021.1892209.

Ramadan MS, Almurshidi AH, Razali SFM, Ramadan E, Tariq A, Bridi RM, Rahman MA, Albedwawi S, Alshamsi M, Alshamisi M, et al. 2025. Spatial decision-making for urban flood vulnerability: a geomatics approach applied to Al-Ain City, UAE. Urban Clim. 59:102297. doi: 10.1016/j.uclim.2025.102297.

Salem ZES, Arafa NA, Abdeldayem AL, Youssef YM. 2025. Machine Learning-Enhanced GALDIT Modeling for The Nile Delta Aquifer Vulnerability Assessment in the Mediterranean Region. Groundw. Sustain. Dev. 101403.

Samany NN, Sheybani M, Zlatanova S. 2021. Detection of safe areas in flood as emergency evacuation stations using modified particle swarm optimization with local search. Appl. Soft Comput. 111:107681. doi: 10.1016/j.asoc.2021.107681.

Sarkar D, Saha S, Mondal P. 2022. GIS-based frequency ratio and Shannon's entropy techniques for flood vulnerability assessment in Patna district, Central Bihar, India. Int J Environ Sci Technol. 19(9):8911–8932. doi: 10.1007/s13762-021-03627-1.

Sarkar D, Mondal P. 2020. Flood vulnerability mapping using frequency ratio (FR) model: a case study on Kulik river basin, Indo-Bangladesh Barind region. Appl Water Sci. 10(1):17. doi: 10.1007/s13201-019-1102-x.

Sepehri M, Malekinezhad H, Jahanbakhshi F, Ildoromi AR, Chezgi J, Ghorbanzadeh O, Naghipour E. 2020. Integration of interval rough AHP and fuzzy logic for assessment of flood prone areas at the regional scale. Acta Geophys. 68(2):477–493. doi: 10.1007/s11600-019-00398-9.

Seydi ST, Kanani-Sadat Y, Hasanlou M, Sahraei R, Chanussot J, Amani M. 2022. Comparison of machine learning algorithms for flood susceptibility mapping. Remote Sens. 15(1):192. doi: 10.3390/rs15010192.

Sharma A, Nerkar S, Banyal R, Poonia M, Kadaverugu R, Damahe L, Tügel F, Holzbecher E, Hinkelmann R. 2024. Comprehensive evaluation of machine learning algorithms for flood susceptibility mapping in Wardha River sub-basin, India. Acta Geophys. 73(3):2725–2748. doi: 10.1007/s11600-024-01471-8.

Yariyan P, Avand M, Abbaspour RA, Torabi Haghighi A, Costache R, Ghorbanzadeh O, Janizadeh S, Blaschke T. 2020. Flood susceptibility mapping using an improved analytic network process with statistical models. Geomat Nat Haz Risk. 11(1):2282–2314. doi: 10.1080/19475705.2020.1836036.

Youssef AM, Pradhan B, Dikshit A, Mahdi AM. 2022. Comparative study of convolutional neural network (CNN) and support vector machine (SVM) for flood susceptibility mapping: a case study at Ras Gharib, Red Sea, Egypt. Geocarto Int. 37(26):11088–11115. doi: 10.1080/10106049.2022.2046866.

Yu H, Luo Z, Wang L, Ding X, Wang S. 2023. Improving the accuracy of flood susceptibility prediction by combining machine learning models and the expanded flood inventory data. Remote Sens. 15(14):3601. doi: 10.3390/rs15143601.

Zeng T, Jin B, Glade T, Xie Y, Li Y, Zhu Y, Yin K. 2024. Assessing the imperative of conditioning factor grading in machine learning-based landslide susceptibility modeling: a critical inquiry. CATENA. 236:107732. doi: 10.1016/j.catena.2023.107732.

Zeng T, Yin K, Gui L, Peduto D, Wu L, Guo Z, Li Y. 2023. Quantitative risk assessment of the Shilongmen reservoir landslide in the Three Gorges area of China. Bull Eng Geol Environ. 82(6):214. doi: 10.1007/s10064-023-03242-z.

Zhang W, Li H, Li Y, Liu H, Chen Y, Ding X. 2021. Application of deep learning algorithms in geotechnical engineering: a short critical review. Artif Intell Rev. 54(8):5633–5673. doi: 10.1007/s10462-021-09967-1.

Zhu K, Wang Z, Lai C, Li S, Zeng Z, Chen X. 2024. Evaluating factors affecting flood susceptibility in the Yangtze river delta using machine learning methods. Int J Disaster Risk Sci. 15(5):738–753. doi: 10.1007/s13753-024-00590-6.